Surface-enhanced Raman scattering study of the adsorption of the anthraquinone pigment alizarin on Ag nanoparticles. J Raman Spectrosc

ARTICLE *in* JOURNAL OF RAMAN SPECTROSCOPY · OCTOBER 2004

Impact Factor: 2.67 · DOI: 10.1002/jrs.1228

4 AUTHORS, INCLUDING:

Maria Vega Cañamares
Spanish National Research Council
27 PUBLICATIONS **698** CITATIONS
SEE PROFILE

José Vicente García-Ramos
Spanish National Research Council
177 PUBLICATIONS **3,785** CITATIONS
SEE PROFILE

S. Sanchez-Cortes
Spanish National Research Council
192 PUBLICATIONS **4,186** CITATIONS
SEE PROFILE

JOURNAL OF RAMAN SPECTROSCOPY
J. Raman Spectrosc. 2004; **35**: 921–927
Published online 25 August 2004 in Wiley InterScience (www.interscience.wiley.com). DOI: 10.1002/jrs.1228

JRS

Surface-enhanced Raman scattering study of the adsorption of the anthraquinone pigment alizarin on Ag nanoparticles

M. V. Cañamares, J. V. Garcia-Ramos, C. Domingo and S. Sanchez-Cortes*

Instituto de Estructura de la Materia, CSIC, Serrano 121, 28006-Madrid, Spain

Received 16 January 2004; Accepted 21 April 2004

FT-Raman and surface-enhanced Raman scattering (SERS) spectroscopy were applied in the vibrational characterization and study of the adsorption and acidity behavior of the highly fluorescent anthraquinone dye alizarin on Ag colloids prepared by chemical reduction with hydroxylamine hydrochloride. The SERS spectra were obtained at different conditions of pH, excitation wavelength and pigment concentration in order to deduce the adsorption mechanism of this molecule. On the basis of the results found we propose an adsorption model for alizarin, which has a different acidic behavior on the metal surface to that in solution. On the metal the deprotonation order of the OH groups changes with respect to the aqueous solution, the OH in position 1 being the first to be ionized instead of that in position 2 as occurs in solution. The two main alizarin forms identified on the metal surface correspond to the mono- and dianionic alizarin species. Copyright © 2004 John Wiley & Sons, Ltd.

KEYWORDS: alizarin; surface-enhanced Raman scattering; adsorption; pigment; dye

INTRODUCTION

Hydroxyanthraquinones have attracted the attention of many researchers owing to their many possible applications related to their interesting photoactivity. Most applications are based in their chromatic properties. Their colors depend on the position and number of hydroxyl substituents.[1]

In particular, dihydroxyquinones have important applications as a prominent family of pharmaceutically active and biologically relevant chromophores. Further, many of them have been used as an analytical tool for the determination of metals, and in electrochemistry.[2]

Alizarin (1,2-dihydroxyanthraquinone) (AZ) (Fig. 1) is extracted from the roots of *Rubia tinctorum* L., where it is the main coloring matter. In addition, it can be found in other types of madder in varying amounts.[3] It is the most important constituent of the madder lake dye, which is a pigment precipitated on to an inert inorganic substrate ($Al_2O_3 \cdot nH_2O$).[1] AZ is of interest both as a pigment and as a biologically active molecule.

As a dye, AZ has been extensively employed in Asia since ancient times for dyeing textile materials. Madder was used as early as the sixteenth century BC in Egypt for dyeing, but madder lake was not found in painting materials until the Roman period. It is rarely found in the European cultural heritage of the Middle Ages, but in the seventeenth and eighteenth centuries its use in paintings increased. Today, AZ is found in artists' paints as synthetic madder.[3]

As a biologically active molecule, AZ has remarkable antigenotoxic activity, because it is an inhibitor of the human recombinant cytochrome P450 isozymes, like other anthraquinone dyes. These isozymes are related to the tumoral activation of many carcinogens such as heterocyclic amines and polycyclic aromatic hydrocarbons. AZ as a component of food can act against the action of these carcinogens.[4]

AZ is highly fluorescent and practically insoluble in water. These properties seriously limit the application of Raman spectroscopy to carry out a structural study of this molecule, although several Raman studies on AZ can be found in the literature.[5] However, Fourier transform (FT) Raman and surface-enhanced Raman scattering (SERS) spectroscopy can be employed in the characterization of this molecule in aqueous media. FT-Raman spectroscopy can be

*Correspondence to: S. Sanchez-Cortes, Instituto de Estructura de la Materia, CSIC, Serrano 121, 28006-Madrid, Spain.
E-mail: imts158@iem.cfmac.csic.es
Contract/grant sponsor: Dirección General de Investigación (Ministerio de Ciencia y Tecnología); Contract/grant number: BFM2001-2265.
Contract/grant sponsor: Comunidad Autonoma de Madrid; Contract/grant number: 07G/0042/2003-1.
Contract/grant sponsor: Red Temática del Patrimonio Histórico (CSIC).

JRS

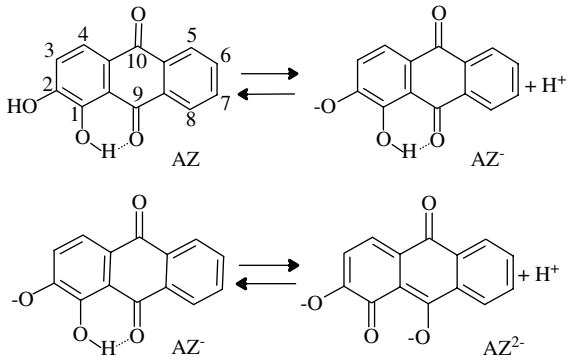

Figure 1. Structure of AZ and acid–basic equilibria in solution.

applied in the Raman study of AZ since the near-infrared excitation lines lie far from its absorption region. The SERS technique involves the use of rough metal surfaces to enhance the Raman emission.[6,7] This technique can be successfully applied in the study of poorly soluble compounds in water, since very low concentrations are required, with the additional advantage of the fluorescence quenching that occurs on the metal surface.[7] In fact, alizarin has been identified in madder lake of the Roman period by SERS after extraction of the dye from its mineral support.[8]

In recent work we have studied the adsorption and acidic behavior of other anthraquinone derivatives.[9,10] In this paper we report a study of the adsorption and the acidic behavior of AZ on silver nanoparticles. To accomplish this we carried out a SERS study at different pH values, excitation wavelengths and adsorbate concentrations. The assignment of the vibrational spectra of alizarin was assisted by a theoretical calculation of the pigment vibrational normal modes.

EXPERIMENTAL

Materials

AZ (97%) was purchased from Acros. Stock solutions of the dye were prepared in 0.5 M sodium hydroxide solution at a concentration of 10^{-2} M. All the reagents employed were of analytical grade and purchased from Sigma and Merck. Aqueous solutions were prepared using triply distilled water. Silver colloids were prepared by reduction of silver nitrate with hydroxylamine hydrochloride.[11] The colloids were activated before adding AZ. This activation consisted in partial aggregation of the colloidal particles and, to accomplish this, 20 µl of 0.5 M potassium nitrate solution were added to 0.5 ml of the Ag colloid. This activation is a prerequisite for SERS spectra to be observed at a higher intensity, as we have demonstrated in other works.[12,13] Then, different volumes of the alkaline aqueous solution of AZ were added to the pre-aggregated colloid to obtain the desired final concentration. Nitric acid and sodium hydroxide were employed to vary the pH value; in these cases no nitrate was added, since the nitric acid and the hydroxide also induced colloid aggregation.

The solid sample for FT Raman spectroscopy was prepared by putting the powdered compounds in a metal holder. In the case of the IR spectrum, the solid alizarin was dispersed in KBr pellets.

Samples for UV–visible spectroscopy in water were prepared by adding an aliquot of the dye dissolved in 0.1% (v/v) aqueous dimethyl sulfoxide (DMSO) up to a concentration of 10^{-5} M. Quartz cells of 1 cm optical path were used.

Instrumentation

The SERS spectra with excitation in the visible region were recorded with a Jobin-Yvon U-1000 spectrophotometer by using 514.5 nm radiation from a Spectra-Physics Model 165 argon ion laser. Slits were set at 4 cm^{-1} and a 90° geometry was used to record the data. The laser power at the sample was ~30 mW. All the spectra were recorded at 1 cm^{-1} step intervals with an integration time of 1 s. The SERS spectrum obtained at 785 nm was measured with a Renishaw RM1000 micro-Raman instrument and a ×50 objective. The laser power at the sample was 2 mW. The resolution was set at 4 cm^{-1} and the geometry of micro-Raman measurements was 180°. The micro-Raman measurements were performed by putting the nanoparticle suspension in a glass slide provided with a groove in the center and covered with a 0.4 mm wide glass cover slide.

FT-Raman and SERS spectra were obtained by using a Bruker RFS 100/S spectrometer. Radiation of 1064 nm from an Nd:YAG laser was used for excitation. The resolution was set to 4 cm^{-1} and a 180° geometry was employed. The output laser power was 150 mW in the case of SERS and solution measurements and 50 mW for the solid samples.

FTIR transmission spectra were recorded with a Bruker IFS 66 instrument. The spectral resolution was 8 cm^{-1} and 100 scans were obtained from each sample.

UV–visible absorption spectra were recorded with a Cintra 5 spectrometer. The samples were put in 1 cm optical path cells.

Calculations

The geometry optimization and theoretical calculations of normal vibrational modes were carried out by using the Gaussian 98 package of programs[14] and employing the B3LYP/6–31G* basis set of the DFT method.

RESULTS AND DISCUSSION

UV–visible spectra of alizarin

Figure 2 shows the absorption spectra of alizarin in DMSO–water (1:1000, v/v). In aqueous medium AZ can exist in the pH range 3.8–12.8 in three different forms, AZ, AZ^- and AZ^{2-} (Fig. 1), corresponding to the absorption maxima at 433 nm (AZ), 526 nm (AZ^-) and 567 and 606 nm

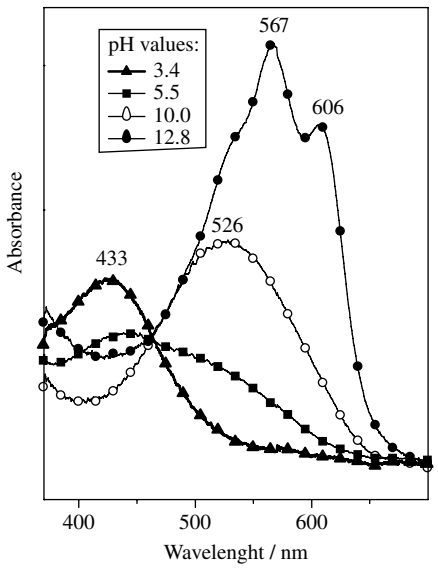

Figure 2. UV–visible spectra of AZ (10^{-5} M) at different pH values.

(AZ^{2-}). The pK values corresponding to the AZ dissociation were deduced from the absorption spectra shown in Fig. 2 by using the graphical method described by Kuban and Havel.[15] The pK values deduced for AZ were $pK_1 = 5.25$ and $pK_2 = 11.5$. These values are lower than those deduced for AZ by Miliani *et al.*[1] in dioxane–water (1 : 2, v/v) solution ($pK_1 = 6.57$ and $pK_2 = 12.36$). The differences in pK values are attributed to the different solvents used to dissolve AZ. The first step in the deprotonation process involves the free hydroxyl group, i.e. that at position 2 (Fig. 1). Nevertheless, the second ionization seems to induce a change in the C═O groups towards position 1, in order to shift the second negative charge in position 9, which is the furthest position in relation to the first one.

Normal Raman and infrared spectra of alizarin and normal mode calculation

The Raman and IR spectra of AZ are shown in Fig. 3(a) and (c), respectively, and the corresponding calculated vibrational spectra in Fig. 3(b) and (d). The main wavenumbers of these spectra and the assignments derived from calculation are displayed in Table 1. In general, there is good concordance regarding the experimental and theoretical Raman and IR peak intensities and positions, except for some bands corresponding to the keto and phenol groups.

The main mismatch between theoretical calculations and experimental spectra arose from the bands corresponding to O–H and C═O stretching modes (at 3624–3544 and 1685/1674 cm^{-1}, respectively), which are shifted downwards in both the experimental Raman and IR spectra. This mismatch is due in part to the fact that theoretical data are obtained from isolated molecules, whereas in the solid state AZ undergoes inter- and intramolecular interactions involving both keto and phenol groups, as was observed in

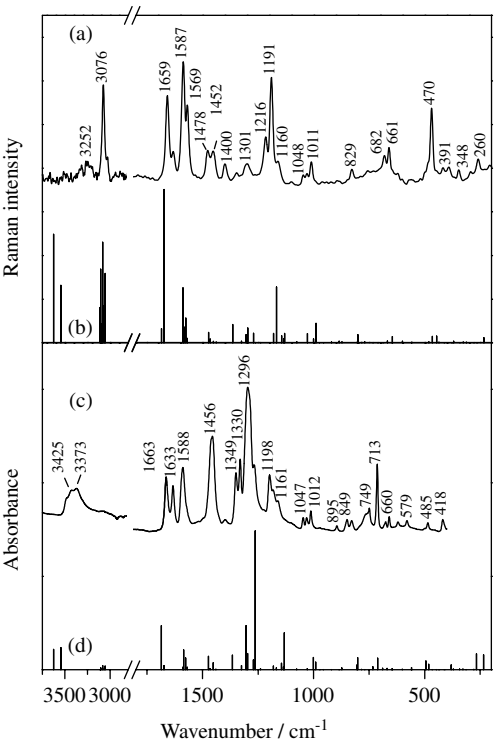

Figure 3. (a) Raman spectrum of solid AZ; (b) theoretical Raman spectrum deduced from DFT calculations; (c) absorption IR spectrum of AZ in KBr; (d) theoretical IR spectrum deduced from DFT calculations.

the case of other anthraquinone derivatives,[9,10] and to the fact that the O–H and the C═O stretching vibrations are strong anharmonic modes.

SERS spectra at different pH values

Figure 4(c)–(e) show the SERS spectra of AZ at different pH values with 1064 nm excitation compared with the normal Raman spectra of the solid [Fig. 4(a)] and an aqueous alkaline solution [Fig. 4(b)]. Neither of the SERS spectra are similar to those of the solid or the DMSO solution, where AZ is supposed to be in the neutral form. This result indicates that AZ is always ionized on the metal surface, even at acidic pH. Surprisingly, there is a greater similarity between the SERS spectrum obtained under acidic conditions and the Raman spectrum of the alkaline aqueous solution [Fig. 4(b)]; at this pH intense peaks at 1627, 1549, 1460/1451, 1327, 1291, 1185 and 1049 cm^{-1} are observed, which correspond to the bands seen at 1624, 1538, 1461, 1323, 1282, 1190 and 1044 cm^{-1} in the Raman spectrum of AZ in alkaline solution. This result suggests that when the molecule is adsorbed on the metal surface the interaction takes place through the keto + hydroxyl groups at positions 9 and 1, corresponding to the A form indicated in Fig. 5(a). Therefore, the interaction with the metal surface induces deprotonation of OH group at position 1 rather than at position 2, as occurs in solution, leading to a large electronic delocalization in the aromatic

Table 1. Main experimental and calculated Raman wavenumbers (cm^{-1}) of alizarin spectra and assignments derived from the calculation

	Normal Raman[a]		SERS[a]				
IR[a] KBr pellet	Solid	Alkaline solution	pH 5.5	pH 11.8	Calculated	Assignments[b]	AZ form
3466w						ν(OH)	
3425m					3624	ν(OH)	
3373m	3252vw				3544	ν(OH)	
3073vw	3076s				3083	ν(CH)	
	3027sh				3055	ν(CH)	
1663m	1659s				1685	ν(C=O)/δ(CCC)	
1633m	1632w	1624s	1627w		1674	ν(C=O)	A
1588m	1587vs			1600m	1588	ν(CC)	B
					1585		
	1569s				1568	ν(CC)	
		1538w	1549s	1543m		ν(CC)	A
				1504m		ν(CC)	B
	1478w	1461vs	1466sh		1473	ν(CO)/ν(CC)/δ(CH)	A
1456s	1452w		1451s	1458m	1452	ν(CC)/δ(COH)/δ(CH)	A
		1425vw	1424w	1423vs			B
1398vw	1400w	1382m	1396w		1439	ν(CC)/δ(CH)	A
1349m	1345vw				1365	ν(CC)/δ(COH)	
1330m		1323m	1327m	1320w	1325	ν(CC)	A
	1301w				1304	ν(CO)/ν(CC)/δ(COH)	
1296vs		1282vs	1291s	1296vs	1297	ν(CO)/ν(CC)/δ(CCC)	A/B
1268m		1258s	1268sh	1272sh	1262	ν(CO)/ν(CC)	B
1224w	1216w	1209vw		1210w	1239	δ(CH)/δ(CCC)	B
1198m	1191s	1190s	1185m	1186w	1181	ν(CC)/δ(CH)/δ(CCC)	A
1161w	1160w			1157w	1167	ν(CC)/δ(CH)	
1047w	1048vw	1044s	1049w	1048w	1076	δ(CCC)	A
1031vw	1031vw				1028	ν(CC)/δ(CH)	
1012w	1011w		1015vw	1018w	1001	ν(CC)/δ(CCC)	B
895vw		901vw	897vw	903vw	886	γ(C–H)	
849w					873	δ(C=O)/δ(CCC)	
828w	829vw	828w	827vw		805	γ(C–H)/γ(C–O)	A
				818vw	802	ν(CC)	B
764w			762w	764vw	770	γ(C–H)/γ(C=O)/τ(CCCC)	
749w					733	δ(CCC)	
713m	682vw	679vw	682m		689	γ(C=O)/γ(C–O)	A
660w	661w	658m	662w	664vw	669	γ(C=O)/δ(CCC)	B
			632m	634w	646	Skeletal vibrations	
619vw					601		
579vw			582m	577w	561		A
		496m	496w	506m	595		B
485vw			478m	481w	482		A
	470s	473w			466		
418w	418vw	417m	421w		413		A
	391vw		392w	398m	380		B
	348vw	336vw	343vs	344m	342		A
	295vw		311w		314		B
			260s			ν(Ag–Cl)	

[a] vw, Very weak; w, weak; m, medium; s, strong; vs, very strong; sh, shoulder.

[b] ν, stretching; δ, in-plane bending; γ, out-of-plane bending; τ, torsion.

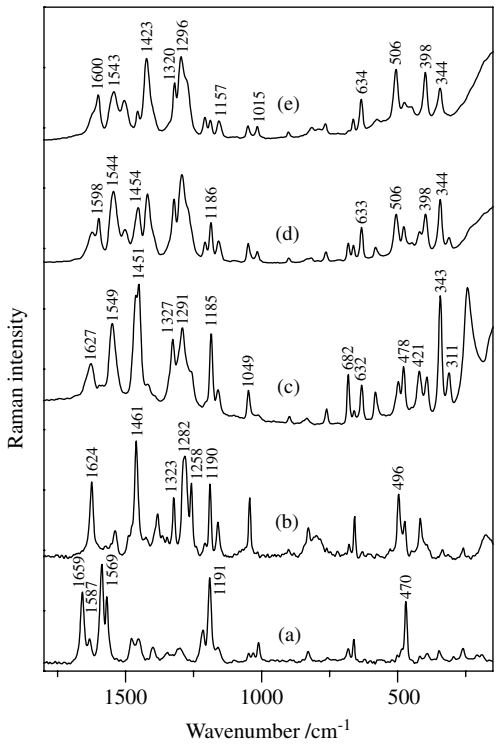

Figure 4. (a) FT-Raman spectrum of AZ in powder; (b) FT-Raman spectrum of AZ in aqueous alkaline solution (pH 13.0); SERS of AZ (10^{-5} M) at pH (c) 5.5, (d) 6.1 and (e) 11.8 in an Ag hydroxylamine colloid. Excitation at 1064 nm.

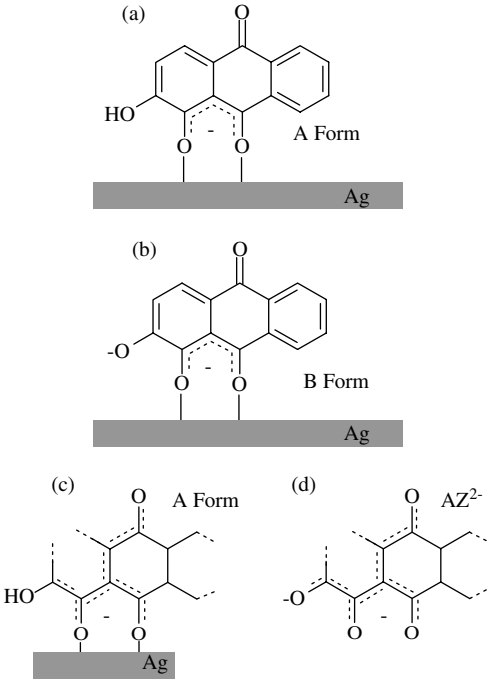

Figure 5. Adsorption mechanism deduced for AZ on Ag surfaces: (a) A form; (b) B form; and similarities of the electronic resonance in (c) adsorbed A form and (d) AZ^{2-}.

moiety indicated in Fig. 5(c), and to a structure which is very similar to the dianionic AZ^{2-} form of the alkaline solution [Fig. 5(d)].

On increasing the pH to 6.1 [Fig. 4(d)] and 11.8 [Fig. 4(e)], an enhancement of the bands at 1600, 1504, 1423, 1272 (shoulder), 1210, 1157, 1015, 634, 506 and 398 cm^{-1} is seen. None of these bands is seen either in the spectrum of the solid or in that of the aqueous alkaline or DMSO solutions. Therefore, we suggest that they correspond to the dianionic B form species in Fig. 5(b), where a second deprotonation of the OH at position 2 occurs. A fact that supports such a conclusion is the downward shift undergone by higher wavenumber bands, whereas the lower ones are shifted upwards. Further, most of the latter bands are related to the C═O and OH groups, which are sensitive to molecular deprotonation. Again, the strong interaction with the metal induces a large delocalization on the dianionic AZ structure, which is the responsible for the observed band shifts.

Hence AZ could change the deprotonation order when adsorbed on the Ag surface in order to interact with the metal through a mechanism similar to the formation of alizarin/Al^{3+} lakes,[16,17] where an interaction between O atoms at positions 1 and 9 with the metal is also proposed.

SERS spectra excited with different excitation wavelengths

Figure 6 shows the SERS spectra of AZ obtained by using different excitation wavelengths and at pH 6.1. The spectra seem to have contributions from both the A and B forms. The relative intensity of the bands at 1460, 1430 and 1324 cm^{-1} is notably increased as the wavelength is decreased, whereas the bands below 700 cm^{-1} are weakened owing to lower coupling of the corresponding vibrational transitions with the electronic transitions when excited with more energetic radiation. On going from the near-IR (1064 nm) to the visible (514.5 nm) region, a significant intensity increase is observed for the bands corresponding to the A form. This is the case, for instance, with the bands at 1617, 1507, 1460 and 1324 cm^{-1}, which are attributed to a higher resonant enhancement of this form in the visible region associated with the AZ^{-}–Ag complex in Fig. 5(a).

SERS spectra at different concentrations

According to the results shown above, at pH 6.1 AZ is adsorbed on the metal surface in two different forms: A and B (Fig. 5). The relationship of these two forms can change with the concentration, as can be seen in Fig. 7, where the spectra of AZ at concentrations of 10^{-6} M [Fig. 7(a)] and 10^{-3} M [Fig. 7(b)] are shown. On decreasing the concentration, relative intensification of the bands corresponding to the B form is observed (e.g. the bands appearing at 1599, 1500, 1422, 1294 and 1015 cm^{-1}). This means that at lower surface

JRS

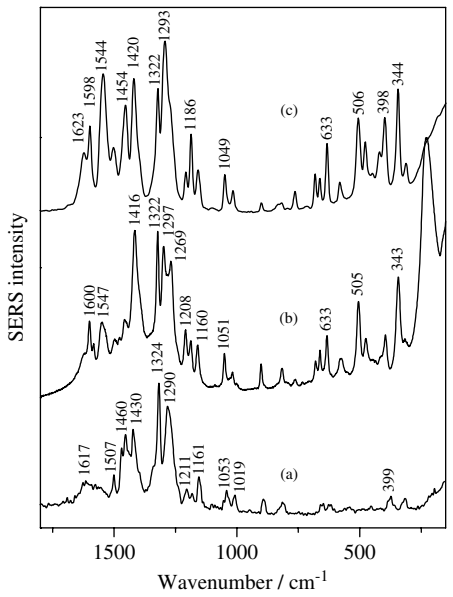

Figure 6. SERS of AZ on an Ag hydroxylamine colloid at different excitation wavelengths: (a) 514.5; (b) 785; (c) 1064 nm. [AZ] = 10^{-5} M, pH = 6.1.

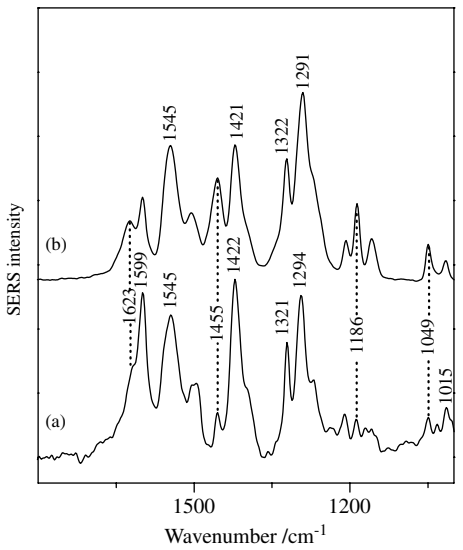

Figure 7. SERS of AZ on an Ag hydroxylamine colloid at (a) 10^{-6} and (b) 10^{-3} M. Excitation at 1064 nm, pH = 6.1.

coverage the AZ molecules are predominantly in the B form because the first adsorption sites occupied by AZ on the metal are those implying double deprotonation of the molecule. This is probably a consequence of the stronger interaction of AZ with the primary adsorption sites, which leads to further deprotonation of the OH at position 2.

A more detailed study of the concentration reveals that the changes observed with the AZ coverage are observed in the 10^{-5}–10^{-6} M concentration range owing to saturation of more active adsorption sites at 10^{-6} M (result not shown). Above the latter concentration, less active adsorption sites start to be occupied by AZ.

CONCLUSIONS

SERS spectroscopy was successfully applied to the study of the vibrational characterization of the highly fluorescent anthraquinone dye alizarin by using Ag nanoparticles. The adsorption mechanism of this molecule was deduced from the SERS spectra obtained at different pH values, indicating that the molecule has a very different acidic behavior on the metal surface to that in solution. On the metal the deprotonation order of the OH groups changes with respect to the aqueous solution, the OH at position 1 being the first to be ionized instead of that at position 2, as occurs in solution. This effect is important since it could affect the dye color when adsorbed on a metallic substrate or when interacting with cations both in solution or when included in a solid matrix such as ormosils (organic modified silicates).

Two main adsorbed AZ forms are identified on the Ag surface, which correspond to chemisorbed monoanionic and dianionic AZ species. The monoanionic form is selectively enhanced by resonance when the excitation wavelength is moved towards higher energies. The SERS spectra at different concentrations demonstrate that the primary adsorption sites for AZ correspond to active sites where AZ is interacting with Ag in its dianionic form, which are occupied at lower surface coverages.

Acknowledgments

This work was supported by the Dirección General de Investigación (Ministerio de Ciencia y Tecnología), project number BFM2001-2265, and Comunidad Autonoma de Madrid, project number 07G/0042/2003-1. This work also received support from the Red Temática del Patrimonio Histórico (CSIC). M.V.C. acknowledges CSIC for an I3P fellowship funded by the European Social Fund.

REFERENCES

1. Miliani C, Romani A, Favaro G. *J. Phys. Org Chem.* 2000; **13**: 141.
2. Thomson RH. *Naturally Occurring Quinones*. Academic Press: New York, 1971.
3. Scheweppe H, Winter J. In *Artists' Pigments. A Handbook of Their History and Characteristics*, vol. 3, FitzHugh EW (ed). Oxford University Press: Oxford, 1998; 109.
4. Takahashi E, Fujita K, Kamataki T, Arimoto-Kobayashi S, Okamoto K, Negishi T. *Mutat. Res.* 2002; **508**: 147.
5. Shoute LCT, Loppnow GR. *J. Chem Phys.* 2002; **117**: 842.
6. Moskovits M. *Rev. Mod. Phys.* 1985; **57**: 783.
7. Creighton JA. In *Spectroscopy of Surfaces*, Clark RJH, Hester RE (eds). Wiley: Chichester, 1988; 37.
8. *Pigments et Colorants de l'Antiquité et du Moyen Age: Teinture, Peinture, Enluminure Études Historiques et Physico-chimiques*. Colloques International du CNRS (Departement des Sciences de l'Homme et de la Societé). Éditions du Centre National de la Recherche Scientifique: Paris, 1990; 249.
9. Jancura D, Sanchez-Cortes S, Kocisova E, Tinti A, Miskovsky P, Bertoluzza A. *Biospectroscopy* 1995; **1**: 265.
10. Fabriciova G, Garcia-Ramos JV, Miskovsky P, Sanchez-Cortes S. *Vib. Spectrosc.* 2002; **30**: 203.

11. Leopold N, Lendl B. *J. Phys. Chem. B* 2003; **107**: 5723.
12. Sanchez-Cortes S, Garcia-Ramos JV, Morcillo G. *J. Colloid Interface Sci.* 1994; **167**: 428.
13. Sanchez-Cortes S, Garcia-Ramos JV, Morcillo G, Tinti A. *J. Colloid Interface Sci.* 1995; **175**: 358.
14. Frisch MJ, Trucks GW, Schlegel HB, Scuseria GE, Robb MA, Cheeseman JR, Zakrzewski VG, Montgomery JA Jr, Stratmann RE, Burant JC, Dapprich S, Millam JM, Daniels AD, Kudin KN, Strain MC, Farkas O, Tomasi J, Barone V, Cossi M, Cammi R, Mennucci B, Pomelli C, Adamo C, Clifford S, Ochterski J, Petersson GA, Ayala PY, Cui Q, Morokuma K, Salvador P, Dannenberg JJ, Malick DK, Rabuck AD, Raghavachari K, Foresman JB, Cioslowski J, Ortiz JV, Baboul AG, Stefanov BB, Liu G, Liashenko A, Piskorz P, Komaromi I, Gomperts R, Martin RL, Fox DJ, Keith T, Al-Laham MA, Peng CY, Nanayakkara A, Challacombe M, Gill PMW, Johnson B, Chen W, Wong MW, Andres JL, Gonzalez C, Head-Gordon M, Replogle ES, Pople JA. *Gaussian 98, Revision A.11*. Gaussian: Pittsburgh, PA, 2001.
15. Kuban V, Havel J. *Acta Chem. Scand*. 1973; **27**: 528.
16. Kiel EG, Heertjes PM. *J. Soc. Dyers Colour* 1963; **79**: 21.
17. Epstein M, Yariv S. *J. Colloid Interface Sci.* 2003; **263**: 377.